www.elsevier.com/locate/developmentalbiology

Somatic mosaicism and allele complexity induced by CRISPR/Cas9 RNA injections in mouse zygotes

Shuo-Ting Yen, Min Zhang, Jian Min Deng, Shireen J. Usman, Chad N. Smith, Jan Parker-Thornburg, Paul G. Swinton, James F. Martin, Richard R. Behringer

PII: S0012-1606(14)00313-3
DOI: http://dx.doi.org/10.1016/j.ydbio.2014.06.017
Reference: YDBIO6469

To appear in: *Developmental Biology*

Received date: 29 April 2014
Revised date: 19 June 2014
Accepted date: 20 June 2014

Cite this article as: Shuo-Ting Yen, Min Zhang, Jian Min Deng, Shireen J. Usman, Chad N. Smith, Jan Parker-Thornburg, Paul G. Swinton, James F. Martin, Richard R. Behringer, Somatic mosaicism and allele complexity induced by CRISPR/Cas9 RNA injections in mouse zygotes, *Developmental Biology,* http://dx.doi.org/10.1016/j.ydbio.2014.06.017

Somatic mosaicism and allele complexity induced by CRISPR/Cas9 RNA injections in mouse zygotes

Shuo-Ting Yen[a,b], Min Zhang[c], Jian Min Deng[b], Shireen J. Usman[b], Chad N. Smith[d], Jan Parker-Thornburg[d], Paul G. Swinton[e], James F. Martin[a, c, e], and Richard R. Behringer[a,b,*]

[a]Program in Developmental Biology, Baylor College of Medicine; [b]Department of Genetics, University of Texas M.D. Anderson Cancer Center; [c]Department of Molecular Physiology and Biophysics, Baylor College of Medicine; [d]Department of Biochemistry and Molecular Biology, University of Texas M.D. Anderson Cancer Center; [e]Texas Heart Institute, Houston, TX 77030, USA

[*]To whom correspondence should be addressed.

Richard Behringer, Department of Genetics, University of Texas MD Anderson Cancer Center, 1515 Holcombe Blvd., Houston, TX 77030, Tel: 713-834-6327, Fax: 713-834-6339, Email: rrb@mdanderson.org

Key words: Gene targeting, pigmentation, knockout, mosaic, genome editing, melanocyte

Abstract

Tyrosinase is the rate-limiting enzyme for the production of melanin pigmentation. In the mouse and other animals, homozygous null mutations in the *Tyrosinase* gene (*Tyr*) result in the absence of pigmentation, i.e. albinism. Here we used the CRISPR/Cas9 system to generate mono- and bi-allelic null mutations in the *Tyr* locus by zygote injection of two single-guide and *Cas9* RNAs.

Injection into C57BL/6N wild-type embryos resulted in one completely albino founder carrying two different *Tyr* mutations. In addition, three pigmentation mosaics and fully pigmented littermates were obtained that transmitted new mutant *Tyr* alleles to progeny in test crosses with albinos. Injection into *Tyr* heterozygous (B6CBAF1/J x FVB/NJ) zygotes resulted in the generation of numerous albinos and also mice with a graded range of albino mosaicism. Deep sequencing revealed that the majority of the albinos and mosaics had more than two new mutant alleles. These visual phenotypes and molecular genotypes highlight the somatic mosaicism and allele complexity in founders that occurs for targeted genes during CRISPR/Cas9-mediated mutagenesis by zygote injection in mice.

Introduction

The CRISPR-Cas9 system, originally derived from the type II adaptive immune system of *Streptococcus pyogenes*, has been engineered as a simple tool for genome editing in plants and animals (Horvath and Barrangou, 2010; Wiedenheft et al., 2012; Belhaj et al., 2013; Sung et al., 2014; Terns and Terns, 2014). The engineered system consists of two parts: a single-guide RNA (sgRNA) and the CAS9 nuclease. The sgRNA is a chimeric molecule, containing the CRISPR RNA (crRNA) and the transacting RNA (tracrRNA) (Jinek et al., 2012). A 20-nucleotide region within the crRNA is designed to be complementary to the desired target DNA sequence, conferring specificity whereas the tracrRNA is necessary for RNA-CAS9 complex formation. The RNA-CAS9 complex generates double strand breaks (DSBs) that can lead to insertions and deletions (indels) due to imprecise DNA repair by non-homologous end joining (NHEJ). The simplicity of the sgRNA in the CRISPR-Cas9 system makes this approach very attractive as a genome editing tool compared to zinc finger nucleases and TAL effector nucleases (TALEN) (Le Provost et al., 2010; Mussolino and Cathomen, 2012). This system has been rapidly adopted

for use in various model organisms including plants, *C. elegans*, *Drosophila*, zebrafish, *Xenopus tropicalis*, mice, and non-human primates (Bassett et al., 2013; Blitz et al., 2013; Friedland et al., 2013; Hwang et al., 2013; Jiang et al., 2013; Nakayama et al., 2013; Wang et al., 2013; Niu et al., 2014).

In mice, the CRISPR/Cas9 system has been used to generate bi-allelic mutant animals in "one-step" simply by injecting sgRNA and *Cas9* mRNA into pronuclear stage zygotes (Mashiko et al., 2013; Wang et al., 2013; Yang et al., 2013; Sung et al., 2014; Zhou et al., 2014). Furthermore, using multiple sgRNAs targeted to different genes in combination with *Cas9* mRNA, it is possible to mutate multiple genes in a single animal (Wang et al., 2013). It is also possible to use this system to introduce oligonucleotides or gene targeting vectors to create knock-ins or conditional alleles by homology-directed repair (HDR) (Ran et al., 2013; Yang et al., 2013).

To explore the efficiency of the CRISPR/Cas9 system in mice, we focused on a locus that, when mutated, would provide a visual phenotype. Tyrosinase is the rate-limiting enzyme that is required for melanin pigmentation synthesis. Animals deficient for tyrosinase function are albino, lacking pigmentation. Tyrosinase is encoded by the *Tyr* locus. Mice carrying one or two wild-type copies of *Tyr* are fully pigmented, whereas mice that are homozygous for a null allele are albino. Inbred mouse strains that are albino all carry a common G to C transversion in nucleotide 308, resulting in a cysteine to serine change in amino acid 103 that blocks pigment production (Yokoyama et al., 1990). *Tyr* acts cell autonomously within melanocytes. Therefore, genetic mosaics or chimeras composed of *Tyr* wild-type and mutant melanocytes can be assessed by visual inspection (Mintz, 1967; Deol et al., 1986).

In the current study, we mutagenized the *Tyr* locus to visualize the efficiency of the CRISPR/Cas9 genome editing system in mice by RNA injections into the pronuclei of zygotes. We also performed deep sequencing of the resulting mice to analyze the complexity of the alleles generated by this mutagenesis system.

Materials and methods

Generation of *Cas9* mRNA and *Tyr* sgRNA

pX330 was obtained from Addgene (Cambridge, MA) (Cong et al., 2013). Complimentary oligonucleotides (Sigma-Aldrich, St. Louis, MO) containing the *Tyr* sgRNA target sequences (**Fig. 1**) were annealed and cloned into the *Bbs*I site of pX330. These plasmids (pTyr4a and pTyr4b) were then sequenced to verify correct insertion of the target sequences. The DNA template for *Cas9 in vitro* transcription was generated by PCR amplification of pX330, using a forward primer that included a T7 promoter (SY009: 5'-TAATACGACTCACTATAGGGAGAATGGACTATAAGGACCACGAC -3') and a reverse primer (SY010: 5'- GCGAGCTCTAGGAATTCTTAC -3'). *Cas9* mRNA was then synthesized, using the mMESSAGE mMACHINE® T7 Ultra Kit (Life Technologies, Carlsbad, CA) and purified by LiCl precipitation. DNA templates of *Tyr* sgRNAs were also generated by PCR amplification of pTyr4a and Tyr4b, using forward primers that included a T7 promoter (SY043: 5'- TTAATACGACTCACTATAGGTTATGGCCGATAGGTGCAT-3' and SY044: 5'-TTAATACGACTCACTATAGGAGTCTCTGTTATGGCCGAT-3') and a common reverse primer (SY011: 5'- AAAAGCACCGACTCGGTGCC-3'). The *Tyr* sgRNAs were then synthesized using the MEGAshortscript™ T7 Kit (Life Technologies). *Cas9* mRNA and

sgRNAs were dissolved in zygote injection buffer (Tris 1 mM, EDTA 0.5 mM). The integrity of the synthesized RNAs was assessed on denaturing agarose gels.

RNA injections into mouse zygotes

A mixture of *in vitro* transcribed RNA (*Cas9*, *Tyr4a*, *Tyr4b*) was injected into the pronuclei of C57BL/6N inbred or (B6CBAF1/J x FVB/NJ) zygotes, using standard procedures (Behringer et al., 2014). In one experiment, RNAs were injected into the cytoplasm of (B6CBAF1/J x FVB/NJ) zygotes. The concentrations of RNA injected were 5.00 ng/μl (*Cas9*), 6.67 ng/μl (*Tyr4a*) and 6.67 ng/μl (*Tyr4b*). Zygotes that survived the injections were transferred into the oviducts of pseudopregnant foster mothers for development to term.

***Tyr* mutation analysis**

Tail genomic DNA was isolated using standard methods (Behringer et al., 2014). Two approaches were used to identify mutations in the *Tyr* locus in mice resulting from zygote injections. In the initial approach, the region around exon 4 of the *Tyr* locus was amplified by PCR, using two sets of primers: 5'-CCCCAAAGAGGTTACCCACA'- 3' and 5'-ACCGCCCTCTTTTGGAAGTT-3'; 5'-CCATAGCTACTTCCAGTCCTAAGGCTT- 3' and 5'-CTTTATGGGAAGCTGGAAATGGGCT-3'. The first set of primers yields a 215 bp product and the second set of primers yields a 1,230 bp product. The amplified products were purified by phenol/chloroform extraction and ethanol precipitation and TA cloned into pGEM-T Easy (Promega, Madison, WI). Individual clones were sequenced and compared to wild type. At least 7 clones were sequenced from each mouse.

In the second approach, primers were designed to flank 162 bp of the gRNA target region. Genomic DNA was amplified using PCR primers: forward 5'-NNNNNNTGAGCTTTACCTGACTCTTGGAGGT; and reverse 5'-NNNNNNCCCTCTTTTGGAAGTTTACCCAGAA, where Ns represent barcode sequences. PCR amplification was performed using a KAPA HiFi HotStart PCR Kit (Kapa Biosystems, Boston, MA). The cycle conditions were: 95^{o}C 3 min, followed by 98^{o}C 20 sec, 60^{o}C 15 sec, 72^{o}C 15 sec (35 cycles), then 72^{o}C for 1 min and store at 4^{o}C.

PCR products were pooled to generate an Ion Torrent DNA sequencing library using the KAPA Library Preparation Kit for Ion Torrent Platforms (Kapa Biosystems, Inc., Wilmington, MA). DNA sequencing was performed on the Ion PGM^{TM} platform using an Ion 316 chip. A total of 1.47 million reads with an average length of 122 bp were generated for 23 founder mice. Over 99.9% of the sequenced reads were barcoded. Raw reads in FASTQ format were collated by their barcodes and then mapped to the mouse genome sequence (mm9 chr7: 94575915-94616411) using Bowtie2 (Version 2.2.1) (Langmead and Salzberg, 2012) with the following parameters:

bowtie2 -q -5 6 --phred33 --sensitive-local

Genomic variants were discovered using a Bayesian method based program Freebayes (Version 0.9.14) (Garrison and Marth, 2012), with minimum alteration fraction setup at 0.05. The Freebayes program recognized individual genome modification events, including short insertions, deletions and single nucleotide alterations. For more complex events, the alignment information was extracted from the SAM output of Bowtie2. The genomic alteration in each read

was quantified for all of the alleles from individual animals. We then calculated the mutant allele frequency at each position, clustered and sorted the reads by their genomic modification using a hierarchical cluster analysis in R (Version 3.0.2) (R Core Team, 2014) with the following script:

hclust(dist(matrix_of_reads), method="complete")

All the reads were then visualized using R package pheatmap (Version 0.7.7) (www.r-project.org). All the mutation events were reported with a minimum occurrence of 5%.

Results

Generation of mice with targeted *Tyr* mutations by zygote injection using the CRISPR/Cas9 system

The five coding exons of *Tyr* were scanned for potential CRISPR/Cas9 target sequences, using the UCSC Genome Browser (http://genome.ucsc.edu), Custom Track, SpCas9 Mm-targets. Two target sequences within exon 4 of the *Tyr* locus were identified to generate sgRNAs (*Tyr4a* and *Tyr4b*) (**Fig. 1**). *Tyr4a* and *Tyr4b* sequences overlap and are shifted by 8 bases. To increase the likelihood of *Tyr* mutagenesis, we decided to co-inject both sgRNAs. *Try4a* and *Tyr4b* sgRNAs and *Cas9* RNA were synthesized *in vitro* and injected together into mouse zygotes. In the first experiment, the pronuclei of C57BL/6N inbred zygotes were injected, using standard methods. Three injection sessions yielded 33 pups. Among these pups there was one completely albino individual and three pigmentation mosaics with small patches of albino fur (**Fig. 2A, B**). The rest

of the pups were fully pigmented and indistinguishable from C57BL/6N. The recovery of a completely albino pup from *Tyr*$^{+/+}$ zygotes suggests that both wild-type alleles had been mutated to null most likely during early cleavage stages of preimplantation development. In addition, the albino patches of fur in the three mosaics suggest that bi-allelic mutation of the *Tyr* locus had also occurred in a subset of cells perhaps at later stages of preimplantation or postimplantation development compared to the albino. In a second experiment, (B6CBAF1 x FVB/NJ) hybrid zygotes that are heterozygous for a *Tyr* null allele (exon 1, G308C, C103S, Yokoyama et al., 1990) were injected either into pronuclei or the cytoplasm in one injection session. Cytoplasmic injection resulted in a higher rate of zygote lysis (~40%) compared to pronuclear injection. However, both types of injections produced pups. Injections into pronuclei yielded 28 pups from three foster mothers and injections into the cytoplasm of zygotes yielded 12 pups from one foster mother. From the pronuclear injections, three albino progeny (~11%) were recovered. In addition, there were 19 pigmentation mosaics (68%), spanning a full range of mosaicism (i.e. mostly pigmented to predominantly albino) (**Fig. 2C**). Six fully pigmented pups (21%) were also recovered. Similar results were obtained for the cytoplasmic injections. Six of the 12 pups obtained from cytoplasmic injections were albino (50%), four were pigmentation mosaics (33%) and two were fully pigmented (~17%) (**Fig. 2D**). Although the yield of albino pups obtained by cytoplasmic injections appears to be higher than by pronuclear injections, the numbers are too low to make strong conclusions (Horri et al., 2014).

Characterization of CRISPR/Cas9-induced *Tyr* mutations

All of the albino pups (n=10) obtained from C57BL/6N and (B6CBAF1 x FVB/NJ) zygote injections were genotyped for CRISPR/Cas9-induced mutations in exon 4 of the *Tyr* locus. Two

sets of primers were used that flank the target sequences (**Fig. 3A**). One set of primers yields a 215 bp DNA fragment, whereas the second set of primers yields a 1.23 kb fragment. Amplified DNA fragments were subcloned and sequenced. The single albino pup (mouse #14) obtained from the C57BL/6N injections was found to have a three-bp deletion in one allele (#1) and a single bp insertion in another allele (#2), both within the target sequences of exon 4 (**Fig. 3B**). The one bp insertion results in a frameshift and immediate termination codon (H420P, N421X) potentially leading to the expression of a truncated protein. The three bp deletion results in a missense mutation followed by a deletion mutation (I418S, G419Δ) that should maintain the open reading frame. These results suggest that the C-terminal truncation encoded by allele #1 and the two amino acid change encoded by allele #2 lead to a complete loss of pigmentation synthesis.

A variety of mutations within exon 4 at the designed target sequence were identified in the 9 albinos recovered from the *Tyr* heterozygous zygote injections (**Fig. 3C**). The predominant type of mutation that was recovered was a small deletion (varying from one to 17 bp) sometimes associated with flanking base pair changes compared to wild type. Allele #1 in mouse #'s 2 and 16 is a one bp deletion that causes a frameshift and 21 ectopic amino acid residues before termination at position 440. Allele #3 in mouse #30 has a 9 bp deletion that should result in a deletion of three amino acids (API, 416-418). In addition, alleles with larger deletions (485 and 924 bp) were identified. In ~25% of the mutant alleles, sequencing identified DNA insertions (one to 292 bp) associated with base changes. Allele #2 in mouse #34 is a two bp insertion that results in a frameshift and 22 ectopic amino acid residues before termination at position 441. Allele #6 in mouse #30 has a 292 bp insertion from the *Rsl1d1* locus on Chr 16 into the target region. Interestingly, using this assay, three of the albino mice contained more than two new

mutant alleles, suggesting that they were genetic mosaics. Indeed, in one albino (mouse #30) there were five mutant alleles identified. Presumably, this genetic mosaicism was caused by a perdurance of sgRNA/*Cas9* RNA and CAS9 protein during early cleavage stages, acting in different blastomeres. Interestingly, only one wild-type sequence for exon 4 was recovered in nearly 90 clones sequenced for the nine albinos from the (B6CBAF1 x FVB/NJ) zygote injections. This suggests that the *Tyr* allele from FVB/NJ with a mutation in exon 1 may have also been mutated in cis in exon 4.

To investigate the complexity of the *Tyr* mutations in greater detail, we performed a deep sequencing analysis on a subset of the albino and pigmentation mosaic mice born from the (B6CBAF1 x FVB/NJ) zygote injections (n=23). Eight pairs of primers, each with a unique 6 base bar code sequence, were designed that flank the target sequence to yield a 162 bp fragment. PCR was performed on three sets of 7-8 individual animals and then individuals within each set were pooled for sequencing. We focused on a 41 bp region containing the PAM sequences of *Tyr4a* and *Tyr4b* (**Fig. 4A, B**). Approximately 10,000 randomly sampled sequences within the 41 bp region of analysis were clustered according to allele type for each mouse (**Fig. 4A, B**). This provided a simple visual readout of the types and relative frequencies of the *Tyr* mutant alleles in each animal. This allowed an assessment of potential relationships between the various alleles generated within an individual. For example, in albino mouse #32, an initial C to A transversion may have occurred that was maintained in Allele 3 but subsequently evolved into Alleles 2 and 4. However, identical mutations can occur independently, for example mouse #2, allele 1 and mouse #16, allele 1 (**Fig. 3**). Thus, it is also possible that the C to A transversion in Alleles 2 and 4 occurred independently. Allele 1 appears to have been generated independently of the Allele 2/3/4 lineage. A similar analysis was performed for one of the pigmentation

mosaics, mouse #18. In this mouse, 4 alleles appear to have been generated independently of each other. In addition, about 30% of the reads were identical to the reference sequence. This pigmentation mosaic had approximately 25% pigmentation, generally correlating with the number of reference sequence read matches. The percentage of allele types from the 57 alleles identified in this subset of 23 mice, using deep sequencing analysis is shown in **Fig. 4C**. Nearly half of the alleles are small deletions (<16 bp) and about a quarter were complex alleles. Insertions, single bp changes, and larger deletions (>100 bp) were in the minority.

Both *Tyr4a* and *Tyr4b* sequences are unique in mouse genome. CRISPR/Cas9-mediated targeted mutagenesis in the mouse can result in off-target mutations (Yang et al., 2013). Possible off-target sequences within the mouse genome for *Tyr4a* and *Tyr4b* were predicted using the CRISPR Design Tool (http://crispr.genome-engineering.org). *Tyr4a* could potentially recognize 41 off-target sequences that have variable numbers of base mismatches. Only two of these are exonic sites. One exonic off-target sequence resides in *Ttc21a* on Chr 9 with four mismatches (positions 3, 4, 14, and 15). The other exonic off-target sequence resides in *Trpm6* on Chr 19 also with four mismatches (positions 12, 17, 19, and 20). *Tyr4b* could potentially recognize 66 putative off-target sequences that have variable numbers of base mismatches. Four of these are exonic sites. Three exonic off-target sequences reside within *Clasp1*, *Herc1*, and *Slfn14* on Chr 1, 9, and 11, respectively. All have four mismatches (positions 5, 6, 15, and 18); (positions 4, 7, 17, and 19); (positions 7, 11, 16, and 17), respectively. One off-target exonic sequence resides in *Scart2* on Chr 7 with three mismatches (positions 6, 11, and 20). The *Tyr* locus maps to 49.01 cM on Chr 7, whereas *Scart2* maps to 85.29 cM (MGI, http://www.informatics.jax.org).

Germ line transmission of targeted *Tyr* alleles

The three pigmentation mosaics, one male and two females, generated from the C57BL/6N zygote pronuclear injections were bred to albino Swiss Webster mates to test for germ line transmission of the targeted *Tyr* mutations. Albino progeny were born from these crosses for all three mosaics (**Fig. 2E**). Interestingly, in the case of pigmentation mosaic male #1, 17/21 (81%) of the progeny were albino, a result that is significantly greater than the predicted 50% (chi-square test, $p<0.005$) that one would expect in crosses of a *Tyr* heterozygote with an albino (**Fig. 2E**). The albino fur observed in these pigmentation mosaic founders was relatively low. However, albino fur would be generated only if both wild-type alleles were mutated. Thus, it is possible that the pigmented regions of mosaic male #1 were actually heterozygous for targeted *Tyr* mutations. The high percentage of albino progeny observed is consistent with the idea that the germ cells of mosaic male #1 were generated from *Tyr* homozygous mutant and heterozygous cells.

We also tested 8 of the fully pigmented pups obtained from the C57BL/6N zygote injections for germ line transmission of targeted *Tyr* mutations because they could be heterozygotes. One of the eight pigmented pups (mouse #5) screened by crosses with albino Swiss Webster mates yielded albino pups (**Fig. 2F**). PCR, subcloning and sequence analysis by BLAST identified a 412 bp insertion of a sequence that is represented in multiple BAC clones (data not shown).

Discussion

We chose to focus on the *Tyr* locus for CRISPR/Cas9 genome editing by RNA injections into mouse zygotes because it provides a visual and spatial readout of mutagenesis that cannot be appreciated for most genes. An albino pup can be distinguished visually amongst pigmented

progeny on the day of birth because they lack eye pigmentation. In addition, within a week after birth one can instantly assess the efficiency of the mutagenesis by visual inspection of the skin. Indeed, soon after birth we could easily identify albinos and mosaics and the extent of the pigmentation mosaicism.

The CRISPR/Cas system has been used to target the *Tyr* locus in *Xenopus tropicalis* (Blitz et al., 2013; Guo et al., 2014; Nakayama et al., 2013) and zebrafish (Jao et al., 2013). In these vertebrate systems, *in vitro* synthesized RNA was injected into the cytoplasm of one- or one- to two-cell stage embryos. In all of these cases, there was an efficient loss of pigmentation although all of the founders had some level of pigmentation mosaicism. This is in contrast to our findings in the mouse with at least one individual derived from the C57BL/6N (wild type) injections that was completely albino. This may be due to the very rapid development of frog and zebrafish embryos compared to the mouse. In 24 hours after fertilization the *Xenopus* embryo has reached the tailbud stage (Stage 22), whereas the zebrafish embryo has reached the pharyngula stage (Prim-5). In contrast, the mouse zygote has only cleaved once 24 hours after fertilization, resulting in a two-cell stage embryo. In the mouse, there is apparently sufficient time after RNA injection into the zygote to translate sufficient amounts of CAS9 protein to mediate bi-allelic mutagenesis prior to or soon after the first cleavage divisions.

Complete albinism and pigmentation mosaicism provides a direct visual assessment of *Tyr* mutagenesis in the mice resulting from the RNA injections into $Tyr^{m/+}$ zygotes because only one wild-type allele needs to be mutated to block pigmentation synthesis. ~10% of the pups were complete albinos and nearly 70% of the mice were pigmentation mosaics, with a wide range of albino mosaicism. This mosaicism may be what usually occurs when mutating a gene of interest using the CRISPR/Cas9 method (Yang et al., 2013; Sung et al., 2014). Many times a T7E1 or a

Surveyor (CEL1) assay is used initially to identify the relatively small mutations created by CRISPR/Cas9 and NHEJ repair (Cong et al., 2013; Jao et al., 2013; Li et al., 2013; Sung et al., 2014). Such an assay would have identified most of the albinos and pigmentation mosaics resulting from the RNA injections into *Tyr*$^{m/+}$ zygotes (~80% of the mice). Some of our pigmentation mosaics had very few patches of albino fur. It is not clear if these mice would have transmitted the new mutant *Tyr* alleles to progeny. We did not test these mosaics for germ line transmission using albino mates because they were already heterozygous for the FVB/NJ albino allele and crosses would have yielded 50% albino pups. It is likely that a single zygote injection session using the CRISPR/Cas9 method will result in many (perhaps too many) mice carrying new mutations at the desired locus. Thus, logistical decisions will have to be made about how many pedigrees will be developed for analysis when resources are limiting. Confounding this is the allele complexity we found in both the albinos and pigmentation mosaics.

Comparisons between our two approaches for identifying specific mutations reveals advantages and disadvantages for each method. The standard PCR, subclone and sequence approach is straightforward but tedious, time consuming and relatively expensive. In addition, this approach did not identify some of the mutant alleles identified by deep sequencing. However, this standard approach did identify large deletions and insertions missed by the deep sequencing analysis. The deep sequencing approach is also straightforward and quick but requires expensive specialized equipment although the cost of assaying the samples is relatively inexpensive. As mentioned above, the strength of the deep sequencing approach is the ability to assess allele complexity and determine the relative frequency of the mutant alleles in each animal. Some of the alleles that were found using the initial standard genotyping approach were

not identified by the high throughput sequencing analysis because they were present at less than a 5% frequency.

The *Tyr* locus encodes a protein of 533 amino acids (www.uniprot.org). Only 3 natural variants in the mouse have been molecularly defined. These include the classic *albino* mutation (Tyr^{c}, C103S), *himalayan* temperature-sensitive allele ($Tyr^{c\text{-}h}$, H420R), and the *chinchilla* hypomorphic allele ($Tyr^{c\text{-}ch}$, A482T) (Beerman et al., 1990; Kwon et al., 1989; Shibahara et al., 1990; Yokoyama et al., 1990). Radiation and chemical mutagenesis screens have led to the isolation of many deletion and point mutations in *Tyr*, including mutations in exon 4 (www.informatics.jax.org). A wide variety of loss-of-function alleles in the *Tyr* locus were generated in the current study located at the target sequence in exon 4. Some of these alleles potentially provide structure-function information about the tyrosinase protein. For example, if translated, the single bp deletion in allele #2 of albino #14 would truncate the C-terminal region of the tyrosinase protein after amino acid 420. Such a truncation would include the transmembrane domain (UniProt accession number: P11344). In addition, triplet deletions, including allele #1 of mouse #14 and allele #3 of mouse #30 would result in in-frame amino acid deletions/substitutions, potentially generating near full-length proteins that lack tyrosinase activity. Many spontaneous mutations found throughout the human *TYR* gene have been molecularly defined (www.omim.org). Of these there are numerous missense and nonsense mutations located in exon 4.

The CRISPR/Cas9 mutagenesis method can lead to off-target mutations (Fu et al., 2013). In this study, we did not genotype our mice for potential off-target sequence mutations. However, the only pertinent potential off-target sequence relative to *Tyr* would be in *Scart2* because like *Tyr* it also resides on Chr 7. However, *Tyr* and *Scart2* are separated by over 35 cM.

In addition, having three mismatches distributed along the target sequence has been shown to significantly reduce off-target sequence mutagenesis (Yang et al., 2013). Furthermore, because the mouse is a genetic model organism, any potential off-target mutation in *Scart2* caused by *Tyr4a*/*b* would be efficiently recombined during routine outcrosses. The modified *Cas9* genes (e.g. nickase) could be used to minimize off-target effects (Fujii et al., 2014; Shen et al., 2014).

The results presented here demonstrate that targeting the *Tyr* locus is a quick and efficient way to establish the CRISPR/Cas9 technology in one's lab, using relatively standard mouse zygote injection methods and visual genotyping. Our studies highlight the range of somatic mosaicism and likely germline mosaicism that can occur during CRISPR/Cas9-mediated mutagenesis. In addition, under our conditions CRISPR/Cas9 functions sufficiently long enough to generate numerous alleles in one individual that could complicate subsequent studies. We did not test the activity of *Tyr4a* and *Tyr4b* sgRNA separately. Thus, it is not clear if injecting one or overlapping sgRNAs would influence somatic mosaicism and allele complexity. Finally, mutating the *Tyr* locus by CRISPR/Cas9 zygote injections could potentially be used in educational situations. For example, injected zygotes could be screened for loss of eye pigmentation at embryonic day 13.5, providing sufficient time in practical courses to visually assess the activity of the CRISPR/Cas9 system *in vivo*.

Acknowledgements

We thank Luis Cedeño-Rosario and Ângela Saito for helpful discussions and Earnessa Edison for animal care. Supported by National Institutes of Health (NIH) grant NIH grant DE023177 and the Vivian L. Smith Foundation to J.F.M. and NIH grant HD030284, the Ben F. Love Endowment, and the University of Texas MD Anderson Genetics and Genomics Center to

R.R.B. Zygote microinjections and embryos transfers, veterinary resources, and DNA sequencing were supported by NIH grant CA016672.

References

Bassett AR, Tibbit C, Ponting CP, Liu JL. 2013. Highly efficient targeted mutagenesis of Drosophila with the CRISPR/Cas9 system. *Cell Rep* 4:220-8.

Beermann F, Ruppert S, Hummler E, Bosch FX, Müller G, Rüther U, Schütz G. 1990. Rescue of the albino phenotype by introduction of a functional tyrosinase gene into mice. *EMBO J* 9:2819-26.

Behringer RR, Gertsenstein M, Vintersten K, Nagy A. 2014. Manipulating the Mouse Embryo: A Laboratory Manual. Cold Spring Harbor Laboratory Press, New York.

Belhaj K, Chaparro-Garcia A, Kamoun S, Nekrasov V. 2013. Plant genome editing made easy: targeted mutagenesis in model and crop plants using the CRISPR/Cas system. *Plant Methods* 9:39.

Blitz IL, Biesinger J, Xie X, Cho KW. 2013. Biallelic genome modification in F(0) Xenopus tropicalis embryos using the CRISPR/Cas system. *Genesis* 51:827-34.

Cong L, Ran FA, Cox D, Lin S, Barretto R, Habib N, Hsu PD, Wu X, Jiang W, Marraffini LA, Zhang F. 2013. Multiplex genome engineering using CRISPR/Cas systems. *Science* 339:819-23.

Deol MS, Truslove GM, McLaren A. 1986. Genetic activity at the albino locus in Cattanach's insertion in the mouse. *J Embryol Exp Morphol* 96:295-302.

Friedland AE, Tzur YB, Esvelt KM, Colaiácovo MP, Church GM, Calarco JA. 2013. Heritable genome editing in C. elegans via a CRISPR-Cas9 system. *Nat Methods* 10:741-3.

Fu Y, Foden JA, Khayter C, Maeder ML, Reyon D, Joung JK, Sander JD. 2013. High-frequency off-target mutagenesis induced by CRISPR-Cas nucleases in human cells. *Nat Biotechnol* 31:822-6.

Fujii W, Onuma A, Sugiura K, Naito K. 2014. Efficient generation of genome-modified mice via offset-nicking by CRISPR/Cas system. *Biochem Biophys Res Commun* 445:791-4.

Garrison E, Marth G. 2014. Haplotype-based variant detection from short-read sequencing. arXiv:1207.3907 [q-bio.GN].

Guo X, Zhang T, Hu Z, Zhang Y, Shi Z, Wang Q, Cui Y, Wang F, Zhao H, Chen Y. 2014. Efficient RNA/Cas9-mediated genome editing in Xenopus tropicalis. *Development* 141:707-14.

Horii T, Arai Y, Yamazaki M, Morita S, Kimura M, Itoh M, Abe Y, Hatada I. 2014. Validation of microinjection methods for generating knockout mice by CRISPR/Cas-mediated genome engineering. *Sci Rep* 4:4513.

Horvath P, Barrangou R. 2010. CRISPR/Cas, the immune system of bacteria and archaea. *Science* 327:167-170.

Hwang WY, Fu Y, Reyon D, Maeder ML, Tsai SQ, Sander JD, Peterson RT, Yeh JR, Joung JK. 2013. Efficient genome editing in zebrafish using a CRISPR-Cas system. *Nat Biotechnol* 31:227-9.

Jao LE, Wente SR, Chen W. 2013. Efficient multiplex biallelic zebrafish genome editing using a CRISPR nuclease system. *Proc Natl Acad Sci USA* 110:13904-9.

Jiang W, Zhou H, Bi H, Fromm M, Yang B, Weeks DP. 2013. Demonstration of CRISPR/Cas9/sgRNA-mediated targeted gene modification in Arabidopsis, tobacco, sorghum and rice. *Nucleic Acids Res* 41:e188.

Jinek M, Chylinski K, Fonfara I, Hauer M, Doudna JA, Charpentier E. 2012. A programmable dual-RNA-guided DNA endonuclease in adaptive bacterial immunity. *Science* 337:816-21.

Kwon BS, Halaban R, Chintamaneni C. 1989. Molecular basis of mouse Himalayan mutation. *Biochem Biophys Res Commun* 161:252-60.

Langmead B, Salzberg SL. 2012. Fast gapped-read alignment with Bowtie 2. *Nat Methods* 9:357-9.

Le Provost F1, Lillico S, Passet B, Young R, Whitelaw B, Vilotte JL. 2010. Zinc finger nuclease technology heralds a new era in mammalian transgenesis. *Trends Biotechnol* 28:134-41.

Li D, Qiu Z, Shao Y, Chen Y, Guan Y, Liu M, Li Y, Gao N, Wang L, Lu X, Zhao Y, Liu M. 2013. Heritable gene targeting in the mouse and rat using a CRISPR-Cas system. *Nat Biotechnol* 31:681-3.

Mashiko D, Fujihara Y, Satouh Y, Miyata H, Isotani A, Ikawa M. 2013. Generation of mutant mice by pronuclear injection of circular plasmid expressing Cas9 and single guided RNA. *Sci Rep* 3:3355.

Mintz B. 1967. Gene control of mammalian pigmentary differentiation. I. Clonal origin of melanocytes. *Proc Natl Acad Sci USA* 58:344-51.

Mussolino C, Cathomen T. 2012. TALE nucleases: tailored genome engineering made easy. *Curr Opin Biotechnol* 23:644-50.

Nakayama T, Fish MB, Fisher M, Oomen-Hajagos J, Thomsen GH, Grainger RM. 2013. Simple and efficient CRISPR/Cas9-mediated targeted mutagenesis in Xenopus tropicalis. *Genesis* 51:835-43.

Niu Y, Shen B, Cui Y, Chen Y, Wang J, Wang L, Kang Y, Zhao X, Si W, Li W, Xiang AP,

Zhou J, Guo X, Bi Y, Si C, Hu B, Dong G, Wang H, Zhou Z, Li T, Tan T, Pu X, Wang F, Ji S, Zhou Q, Huang X, Ji W, Sha J. 2014. Generation of gene-modified cynomolgus monkey via Cas9/RNA-mediated gene targeting in one-cell embryos. *Cell* 156:836-43.

Ran FA, Hsu PD, Lin CY, Gootenberg JS, Konermann S, Trevino AE, Scott DA, Inoue A, Matoba S, Zhang Y, Zhang F. 2013. Double nicking by RNA-guided CRISPR Cas9 for enhanced genome editing specificity. *Cell* 154:1380-89.

Shen B, Zhang W, Zhang J, Zhou J, Wang J, Chen L, Wang L, Hodgkins A, Iyer V, Huang X, Skarnes WC. 2014. Efficient genome modification by CRISPR-Cas9 nickase with minimal off-target effects. *Nat Methods* 11:399-402.

Shibahara S, Okinaga S, Tomita Y, Takeda A, Yamamoto H, Sato M, Takeuchi T. 1990. A point mutation in the tyrosinase gene of BALB/c albino mouse causing the cysteine----serine substitution at position 85. *Eur J Biochem* 189:455-61.

Sung YH, Kim JM, Kim HT, Lee J, Jeon J, Jin Y, Choi JH, Ban YH, Ha SJ, Kim CH, Lee HW, Kim JS. 2014. Highly efficient gene knockout in mice and zebrafish with RNA-guided endonucleases. *Genome Res* 24:125-31.

Terns RM, Terns MP. 2014. CRISPR-based technologies: prokaryotic defense weapons repurposed. *Trends Genet* 30:111-118.

Wang H, Yang H, Shivalila CS, Dawlaty MM, Cheng AW, Zhang F, Jaenisch R. 2013. One-step generation of mice carrying mutations in multiple genes by CRISPR/Cas-mediated genome engineering. *Cell* 153:910-8.

Wiedenheft B, Sternberg SH, Doudna JA. 2012. RNA-guided genetic silencing systems in bacteria and archaea. *Nature* 482:331-8.

Yang H, Wang H, Shivalila CS, Cheng AW, Shi L, Jaenisch R. 2013. One-step generation of mice carrying reporter and conditional alleles by CRISPR/Cas-mediated genome engineering. *Cell* 154:1370-9.

Yokoyama T, Silversides DW, Waymire KG, Kwon BS, Takeuchi T, Overbeek PA. 1990. Conserved cysteine to serine mutation in tyrosinase is responsible for the classical albino mutation in laboratory mice. *Nucleic Acids Res* 18:7293-8.

Zhou J, Wang J, Shen B, Chen L, Su Y, Yang J, Zhang W, Tian X, Huang X. 2014. Dual sgRNAs facilitate CRISPR/Cas9-mediated mouse genome targeting. *FEBS J* 281:1717-25.

Figure legends

Fig. 1. Mouse *Tyr* gene structure and small guide RNA design. Diagram of mouse *Tyr* locus, showing 5 exons. Two overlapping target sequences in exon 4 were identified to generate two sgRNAs (*Tyr4a* and *b*). PAM sequences are indicated in red. Untranslated regions, gray boxes; protein-coding regions, black boxes.

Fig. 2. Pigmentation phenotypes of mice resulting from *Tyr* CRISPR/Cas9 targeting by RNA injections into zygotes. A, One albino (white arrowhead) and one pigmentation mosaic (yellow arrowhead) in one litter from RNA injections into C57BL/6N zygotes. **B**, Two pigmentation mosaics with small patches of albino fur were found in another litter from injected C57BL/6N zygotes. **C**, **D**, Pups generated from RNA injections of (B6CBAF1/J X FVB/NJ) zygotes into pronuclei (**C**) or cytoplasm (**D**). **E**, Male pigmentation mosaic #1 (yellow asterisk) from the C57BL/6N injections was bred with an albino Swiss female to generate pups. Numerous albino progeny were obtained, demonstrating germ line transmission of the targeted *Tyr* mutant allele. **F**, One of fully pigmented littermates from the C57BL/6N injections (yellow asterisk), a male, was bred with an albino Swiss female (black asterisk). Albino progeny were obtained, demonstrating germ line transmission of the targeted *Tyr* mutant allele.

Fig. 3. Molecular characterization of CRISPR/Cas9-mediated *Tyr* mutations. A, *Tyr4a* and *Tyr4b* target region within exon 4 of the *Tyr* locus (yellow box). Primer sets flanking the target region are shown. One set amplifies a 215 bp fragment (red arrows), whereas a second set amplifies a 1,230 bp fragment (orange arrows). **B**, Two mutant alleles were identified in the

albino mouse resulting from the C57BL/6N zygote injections. Bold sequence, *Tyr4a* and *Tyr4b* target sequence; green sequence, PAM sites; *n*, number of clones sequenced per allele; WT, wild-type reference sequence. **C**, Mutant alleles identified in mice resulting from injections into (B6CBAF1/J x FVB/NJ) zygotes. Red sequence, bp changes or insertions; *Rsl1d1* sequence in allele 6 in mouse #30 was apparently derived from Chr 16.

Fig. 4. High-throughput DNA sequencing of CRISPR/Cas9-induced *Tyr* mutations. A, **B**, Heat map of DNA sequence reads within a 41 bp segment of the CRISPR target sequence, showing patterns of mutant alleles in founder mice. The sequences of the mutant alleles were aligned to the reference mouse genome (Ref). Sequence numbering is relative to the PAM sequence. The sequence and frequency of each allele is shown. **A**, albino mouse #32. **B**, pigmentation mosaic mouse #18. Four different mutant alleles were identified in both mice. **C**, Frequency (and number) of various types of mutations identified by high-throughput DNA sequencing. A total of 57 mutant alleles with at least 5% read coverage was detected in 9 albino and 14 pigmentation mosaic mice. The mutations were categorized as single basepair alteration (alt), deletion (del), insertion (ins), large deletion (bigdel), and complex events (comp).

Yen et al.

Highlights

- CRISPR/Cas was used to mutate the *Tyr* locus of mice by RNA injection.
- Completely albino and a wide range of pigmentation mosaic founders were generated.
- Deep sequencing showed that most founders had >2 new mutant alleles.
- Germline transmission of the mutant alleles was demonstrated.

Figure 1

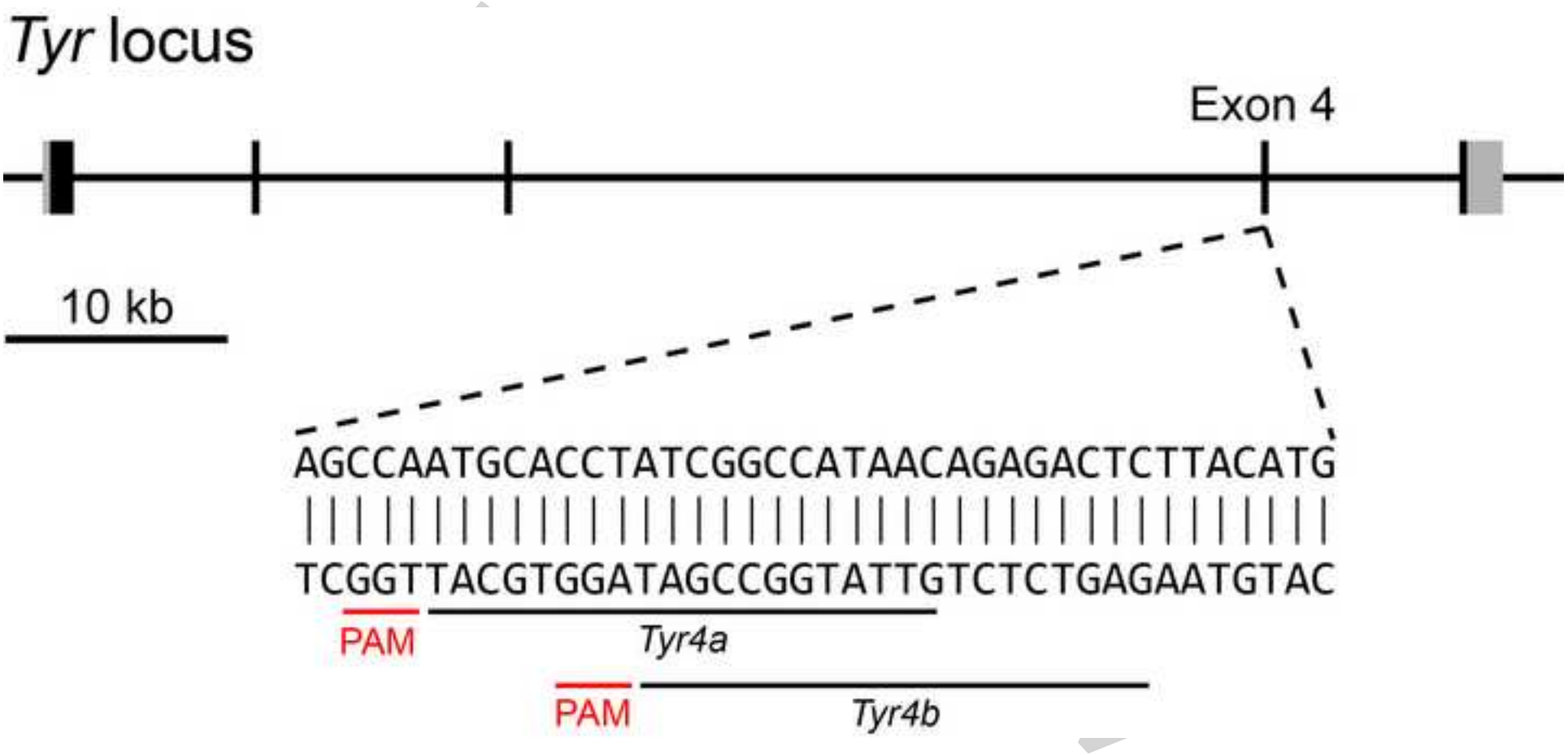

Figure 2

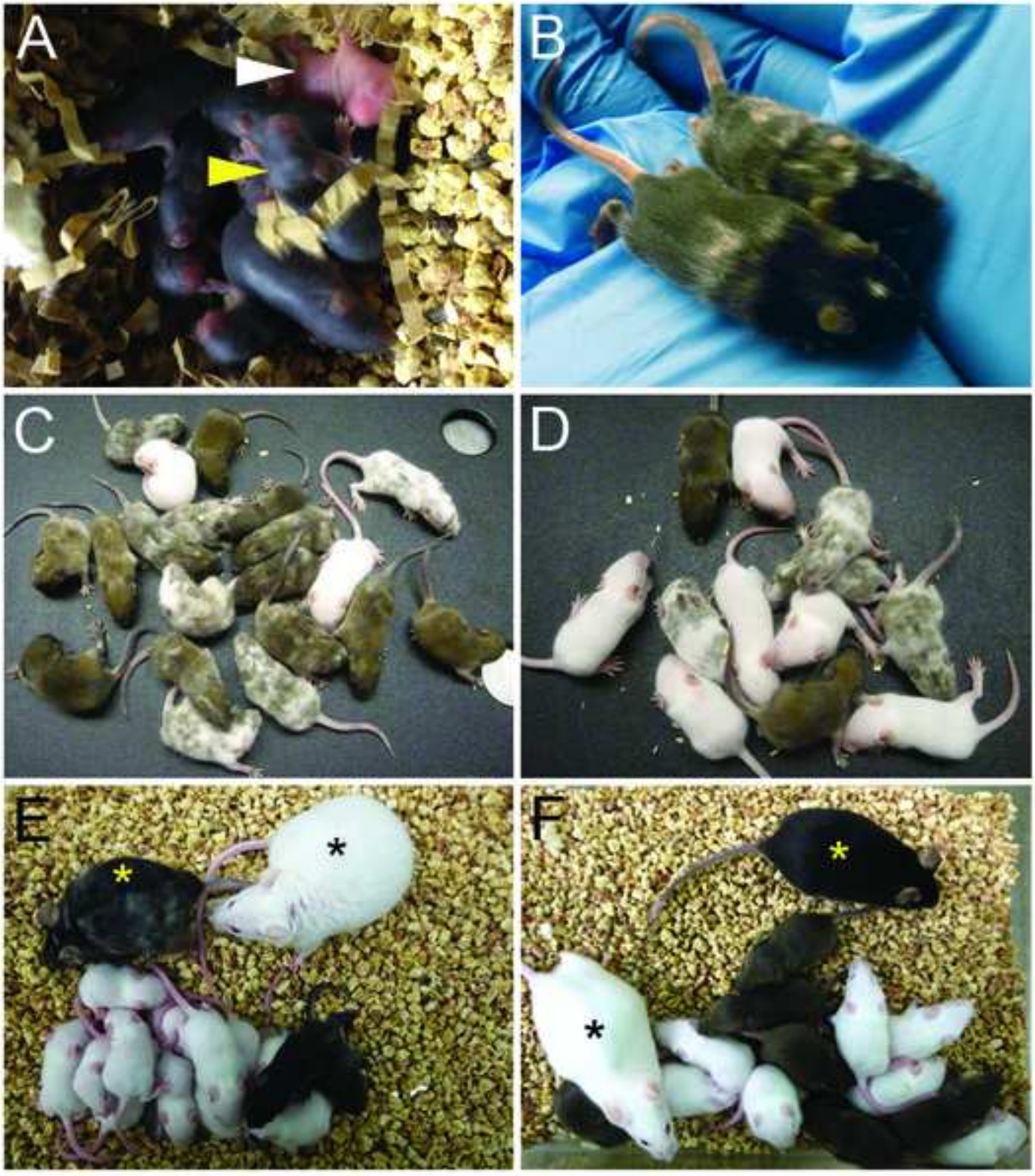

Figure 3

A

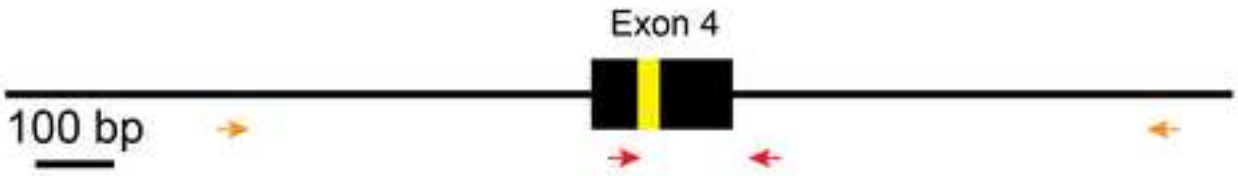

B

C57BL/6N

Mouse		(*n*)
WT	AAGTTTACCCAGAAGCCAATGCACCTATCGGCCATAACAGAGACTCTTACATGGTTC	
14	AAGTTTACCCAGAAGCCAATGCACCTA---GCCATAACAGAGACTCTTACATGGTTC	allele 1 (1)
14	AAGTTTACCCAGAAGCCAATGCACCTATCGGGCCATAACAGAGACTCTTACATGGTTC	allele 2 (11)

C

B6CBAF1/J X FVB/NJ

Deletions

Mouse		(*n*)
WT	AAGTTTACCCAGAAGCCAATGCACCTATCGGCCATAACAGAGACTCTTACATGGTTC	
02	AAGTTTACCCAGAAGCCAATGCACCTATCG-CCATAACAGAGACTCTTACATGGTTC	allele 1 (9)
16	AAGTTTACCCAGAAGCCAATGCACCTATCG-CCATAACAGAGACTCTTACATGGTTC	allele 1 (4)
16	AAGTTTACCCAGAAGCCAATGCA--------CCATAACAGAGACTCTTACATGGTTC	allele 2 (3)
29	AAGTTTACCCAGAA----------GCCATAACAGAGACTCTTACATGGTTC	allele 1 (1)
30	AAGTTTACCCAGAAGCC----------ATAACAGAGACTCTTACATGGTTC	allele 1 (1)
30	AAGTTTACCCAGAAGCCTCTG----TATCGGCCATAACAGAGACTCTTACATGGTTC	allele 2 (3)
30	AAGTTTACCCAGAAGCCAAT---------GGCCATAACAGAGACTCTTACATGGTTC	allele 3 (5)
30	AAGTTTACCCAGAAGCCAAT----------GCCATAACAGAGACTCTTACATGGTTC	allele 4 (1)
31	AAGTTTACCCAGAAGCCAATG-----ATCGGCCATAACAGAGACTCTTACATGGTTC	allele 1 (7)
31	AAGTTTACCCAGAAGCCAAT----------GCCATAACAGAGACTCTTACATGGTTC	allele 2 (1)
32	AAGTTTACCCAGAAGCCAATGAA-------GCC-TATCAGAGGCTCTTACATGGTTC	allele 1(10)
33	AAGTTTACCCAGAAGCCA--------ATCGGCCATAACAGAGACTCTTACATGGTTC	allele 1 (3)
33	AAGTTTACCCAGAAGCCAATGCACCTAT--AACATAACAGAGACTCTTACATGGTTC	allele 2 (6)
34	AAGTTTACCCAGAAGCC----------TATCAGAGACTCTTACATGGTTC	allele 1 (5)
29	485 bp deletion & AGTAATA insertion	allele 2 (9)
30	924 bp deletion	allele 5 (1)

Insertions

Mouse		(*n*)
WT	TACCCAGAAGCCAATGC-------ACCTATC-GG--CCATAACAGAGACTCTTACAT	
27	TACCCAGAAGCCAATGC-------ACCTATCGGG--CCATAACAGAGACTCTTACAT	allele 1 (9)
33	TACCCAGAAGCCAATCAGAAGTTTACCCAGA-AG--CCATAACAGAGACTCTTACAT	allele 3 (1)
34	TACCCAGAAGCCAATGC-------ACCTATC-AGAGCCATAACAGAGACTCTTACAT	allele 2 (5)
34	TACCCAGAAGCCAATGC-------ACCTATC-AGAGCCATAACGGAGACTCTTACAT	allele 3 (1)
30	TACCCAGAAGCCAATGC-------AC-*Rsl1d1*G--CCATAACAGAGACTCTTACAT	allele 6 (3)